

Stereochemical Assignment and Absolute Abundance of Nonproteinogenic Amino Acid Homoarginine in Marine Sponges

Ipsita Mohanty, Samuel G. Moore, Jason S. Biggs, Christopher J. Freeman, David A. Gaul, Neha Garg, and Vinayak Agarwal*



Cite This: *ACS Omega* 2021, 6, 33200–33205



Read Online

ACCESS |



Metrics & More

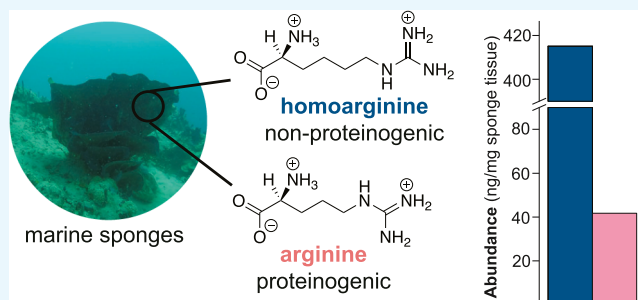


Article Recommendations



Supporting Information

ABSTRACT: Together with arginine, the nonproteinogenic amino acid homoarginine is a substrate for the production of vasodilator nitric oxide in the human body. In marine sponges, homoarginine has been postulated to serve as a precursor for the biosynthesis of pyrrole–imidazole alkaloid and bromotyrosine alkaloid classes of natural products. The absolute abundance of homoarginine, its abundance relative to arginine, and its stereochemical assignment in marine sponges are not known. Here, using stable isotope dilution mass spectrometry, we quantify the absolute abundances of homoarginine and arginine in marine sponges. We find that the abundance of homoarginine is highly variable and can far exceed the concentration of arginine, even in sponges where incorporation of homoarginine in natural products cannot be rationalized. The [homoarginine]/[arginine] ratio in marine sponges is greater than that in human analytes. By derivatization of sponge extracts with Marfey's reagent and comparison with authentic standards, we determine the L-isomer of homoarginine to be exclusively present in sponges. Our results shed light on the presence of the high abundance of homoarginine in marine sponge metabolomes and provide the foundation to investigate the biosynthetic routes and physiological roles of this nonproteinogenic amino acid in sponge physiology.



INTRODUCTION

Homoarginine (**1**, Figure 1A) is a nonproteinogenic amino acid present in the human metabolome. Together with L-arginine (**2**), **1** is a substrate for nitric oxide synthase leading to the production of vasodilator nitric oxide (NO).¹ Due to its role in NO production, the abundance of **1** in the human blood plasma is negatively correlated with cardiovascular risk and renal dysfunction.^{2,3} The abundance of **1** increases during pregnancy with proposed roles in increasing the blood volume and vasodilation.⁴ The enzyme arginine/glycine amidinotransferase catalyzes the amidino group transfer from **2** to the side chain primary amine of lysine (**3**) leading to the production of **1** (Figure 1B).⁵

Although the function of **1** and its relevance as a disease biomarker in mammalian physiology are well validated, the presence, abundance, and role(s) of **1** in other biomes have received lesser attention. We recently reported the detection of **1** in marine sponges.^{6,7} Sponges are benthic invertebrate metazoans and are prolific producers of bioactive small organic molecules called natural products.^{8,9} Molecule **1** was rationalized to be a biosynthetic precursor of bromotyrosine alkaloid natural products¹⁰ aplysinamisine I¹¹ (**4**, Figure 1C) and aerophobin 2¹² (**5**) that are detected in *Aplysina* and *Aiolochoxia* spp. sponges⁷ and a precursor of polybrominated pyrrole–imidazole alkaloid natural products¹³ such as oroidin

(**6**) that are detected in the metabolome of the *Stylissa* sp. sponge (Figure 1C,D).⁶ In concert with the abovementioned biochemical activity of arginine/glycine amidinotransferase which converts **3** to **1**, radiolabeled **3** was found to be incorporated in **6**, conceivably involving the intermediate **1**.^{14,15} The construction of **4**–**6** from **1** is expected to proceed via hydroxylation, followed by oxidative intramolecular dehydration to furnish the aminoimidazole heterocycle akin to enduracididine biosynthesis.^{6,7,16} Some marine sponges such as *Ianthella* sp. that do not possess natural products that can readily be rationalized to be derived from **1** also bear high concentrations of **1**.⁷ The marine sponge eukaryotic host harbors a symbiotic microbiome; the presence of **1** is independent of the microbiome architecture of the sponge holobiont. Although *Aplysina* and *Aiolochoxia* spp. sponges are high microbial diversity and high microbial abundance sponges, *Stylissa* and *Ianthella* spp. are low microbial diversity and low microbial abundance sponges.⁷

Received: October 11, 2021

Accepted: November 16, 2021

Published: November 25, 2021



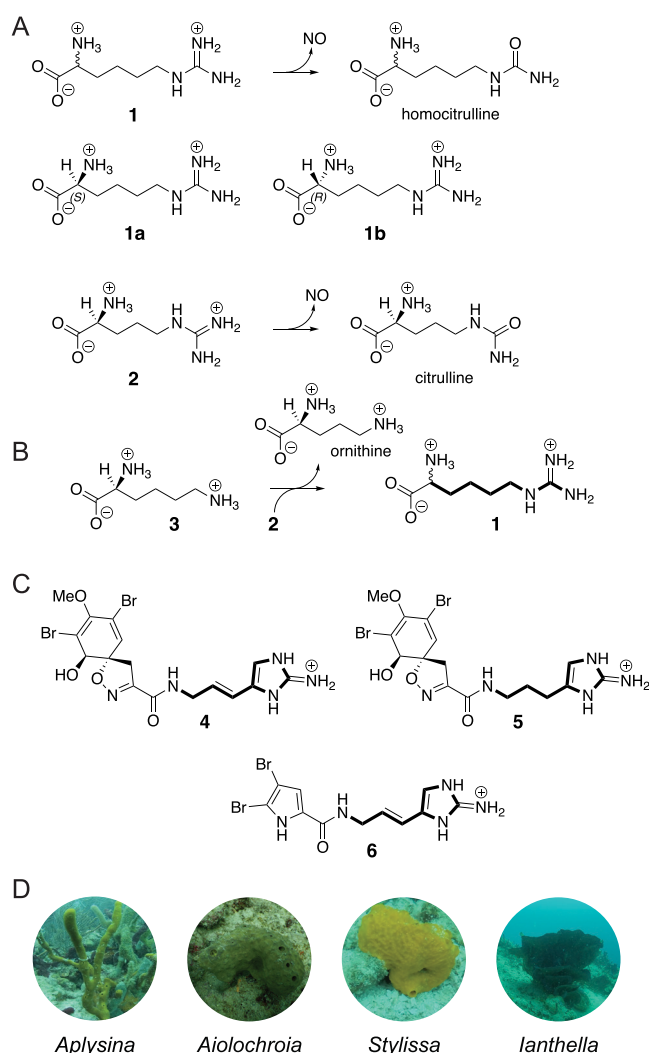


Figure 1. Role and production of **1**. (A) Enzyme NO synthase converts **1** and **2** to NO with concomitant production of homocitrulline and citrulline, respectively. The two possible stereoisomers of **1**, **1a** and **1b**, are shown. (B) Amidinotransfer from **2** to the side chain ϵ -amine of **3** leads to the production of **1** together with the nonproteinogenic amino acid ornithine. (C) Marine sponge-derived natural products in which the incorporation of **1** can be rationalized. (D) Marine sponge samples used in this study. *Aplysina* and *Aiolochroia* spp. sponges were collected in the Florida Keys, and *Stylissa* and *Ianthella* spp. sponges were collected in Guam.

Our prior detection of **1** in marine sponge metabolomes was bereft of the stereochemical assignment as the analytical methods employed did not differentiate between *L*-homocitrulline (**1a**, Figure 1A) and *D*-homocitrulline (**1b**). Moreover, the absolute abundance of **1** in sponge metabolomes was not determined. In this study, we query the stereochemistry at $1\text{-C}\alpha$ and determine the isomer **1a** to be exclusively present in multiple marine sponges. By synthesizing an isotopically labeled standard of **1a** and spiking the standard into sponge tissues, we determine the absolute abundance of **1a** and compare that to the abundance of **2** in *Aplysina*, *Aiolochroia*, *Stylissa*, and *Ianthella* spp. sponges. We find the proteinogenic amino acid **2** to be uniformly abundant in these phylogenetically and geographically dispersed sponges. However, the abundance of **1a** was variable and was found to be several folds higher than **2** even in the *Ianthella* sp. sponge that does not

contain natural products derived from **1**. Our results now set the stage for investigating the physiological role(s) potentiated by the high concentration of **1** in marine sponges.

MATERIALS AND METHODS

Marine Sponges Used in the Study. Phylogeny and natural product chemical classes present in marine sponges used in this study are delineated in Table 1.^{6,7,17}

Table 1. Marine Sponges Used in This Study

sponge genus	collection site	dereplicated natural product chemical class	refs
<i>Aplysina</i>	Florida Keys	bromotyrosine alkaloids	Reference 7
<i>Aiolochroia</i>	Florida Keys	bromotyrosine alkaloids	Reference 7
<i>Stylissa</i>	Guam	pyrrole–imidazole alkaloids	Reference 6
<i>Ianthella</i>	Guam	bromotyrosine alkaloids	References 7 and 17

Synthesis of **1b.** The procedure for synthesis of **1b** was adopted from the literature.¹⁸ Diisopropylamine (1.41 mL, 10.04 mmol) was added to a stirred solution of *D*-*N*- α -Boc-lysine (485 mg, 1.97 mmol) in 10 mL of MeOH at room temperature, followed by the addition of the guanidinylation reagent *N,N'*-bis-Boc-1-guanyl pyrazole (1.63 g, 5.28 mmol). The reaction mixture was stirred at room temperature for 3 h. The reaction mixture was concentrated under vacuum. Deprotection of the Boc functional group was achieved by dissolving the guanidylated product (100 mg) from the previous step in 3 mL of DCM, followed by the dropwise addition of 2 mL of trifluoroacetic acid. The reaction mixture was stirred at room temperature for 16 h and concentrated under vacuum. Cation-exchange chromatography was performed using the DOWEX resin, and the pure molecule **1b** was eluted using 1 M aqueous ammonium hydroxide as the mobile phase. ¹H NMR (Figure S1, 800 MHz, CD₃OD): δ 1.40–1.49 (m, 2H), 1.62 (q, J = 7.4 Hz, 2H), 1.88–1.96 (m, 2H), 3.17 (t, J = 7.0 Hz, 2H), 3.98 (t, J = 6.3 Hz, 1H).

Synthesis of the Isotopic Standard of **1a.** The isotopic standard of **1a** was synthesized based on the literature procedure.¹⁹ To a stirred solution of ¹³C, ¹⁵N-labeled *L*-lysine chloride (61 mg, 0.32 mmol) in 1.2 mL of 1 M NaOH, a solution of CuSO₄ (48 mg, 0.19 mmol) in 3 mL of water was added. The reaction mixture was stirred at room temperature for 5 h. The guanidinylation reagent *N,N'*-bis-Boc-1-guanyl pyrazole (139 mg, 0.45 mmol) and NaHCO₃ (53 mg, 0.63 mmol) were added. The reaction mixture was stirred at room temperature for 24 h. A blue precipitate of cupric–lysine complex was obtained after filtration and was dissolved in saturated ethylenediaminetetraacetic acid and stirred overnight at room temperature. The white precipitate thus obtained was carried forward for deprotection of the Boc groups by acid treatment as abovementioned and characterized using ¹H NMR. ¹H NMR (Figure S2, 800 MHz, D₂O): δ 1.40 (d, J = 51.2 Hz, 2H), 1.52 (d, J = 11.9 Hz, 1H), 1.55–1.63 (m, 3H), 1.73 (tt, J = 8.6, 4.3 Hz, 2H), 1.87 (d, J = 33.4 Hz, 2H), 2.03 (d, J = 33.2 Hz, 2H), 2.23 (s, 1H), 3.12 (tt, J = 7.3, 3.5 Hz, 2H), 3.30 (tt, J = 7.4, 3.6 Hz, 2H), 3.89 (q, J = 5.4 Hz, 1H), 4.08 (q, J = 5.4 Hz, 1H).

Derivatization of Standards and Sponge Extracts. The protocol for derivatizing **1a** and **1b** standards was adapted from the literature.²⁰ To a 50 μ L aqueous solution of 50 mM

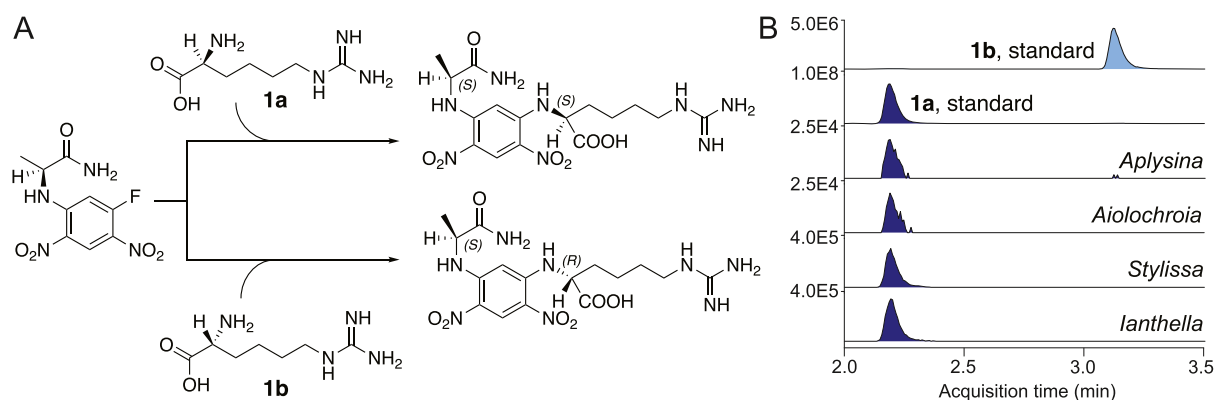


Figure 2. L-isomer of **1** is present in marine sponges. (A) Derivatization of **1a** and **1b** with Marfey's reagent to yield diastereomeric products. (B) EICs $[M - H]^{-}$ m/z 439.17 demonstrating chromatographic separation of derivatized standards of **1a** and **1b**, and comparison with similarly derivatized sponge extracts.

standards, 20 μL of 1 M NaHCO_3 was added, followed by the addition of 100 μL of 1% (w/v) 1-fluoro-2-4-dinitrophenyl-5-L-alanine amide (Marfey's reagent) in acetone. The solution was vortexed and then incubated at 37 $^{\circ}\text{C}$ for 1 h. The reactions were quenched by the addition of 20 μL of 1 N HCl. The samples were diluted by the addition of 810 μL of MeCN and chromatographed on a Thermo Scientific Accucore C_{30} reversed phase LC column (250 \times 2.1 mm, 2.6 μm particle size) coupled to a Thermo Fisher Scientific Orbitrap ID-X Tribrid mass spectrometer operating in the negative ionization mode with an electrospray ionization source. The chromatographic method for sample analysis involved elution with water with 10 mM ammonium acetate and 0.1% acetic acid (mobile phase solvent A) and 90:10 isopropanol/water with 10 mM ammonium acetate (mobile phase solvent B) using the following gradient program: 0 min 8% B; 5 min 25% B; 7 min 90% B; 7.4 min 100% B; 10.5 min 100% B; 10.7 min 25% B; and 12 min 8% B. The flow rate was 0.4 mL/min. The column temperature was set to 40 $^{\circ}\text{C}$, and the injection volume was 0.5 μL . The MeOH extracts of pulverized sponge tissues were derivatized using the same protocol as described above, with the only deviation being the use of 200 μL of sponge extract instead of 50 μL of aqueous solution of standards.

Isotope Standard Spiking in Sponge Tissues. Three biological replicates for each sponge species were used in this study. The isotopic standard for **2** was obtained commercially. In a 2 mL Eppendorf safe-lock tube, lyophilized sponge tissues were homogenized with two tungsten carbide beads in a QIAGEN TissueLyser II at 20 Hz for 20 min, in two cycles of 10 min each. The pulverized sponge tissue was weighed in Eppendorf tubes and known concentrations of stable isotope labeled analytical standards **1a** and **2** were added. The spiked sponge tissues were extracted with 80% MeOH, sonicated for 45 min on ice, and centrifuged at 16 000g for 30 min. The supernatant was transferred to autosampler vials for analysis.

Development of LC-MS/MS Method. LC/MS data were acquired using a Waters Corporation ACQUITY UPLC BEH Amide column (2.1 \times 150 mm, 1.7 μm particle size) coupled to a high-resolution accurate mass Orbitrap ID-X Tribrid mass spectrometer. The chromatographic method for sample analysis involved elution with 20:80 water/MeCN with 10 mM ammonium formate and 0.1% formic acid (mobile phase A) and MeCN and 0.1% formic acid (mobile phase B) using the following gradient program: 0 min 5% A; 0.5 min 5%

A; 8 min 60% A; 9.4 min 60% A; 9.5 min 5% A; and 12 min 5% A. The flow rate was set at 0.4 mL/min. The column temperature was set to 40 $^{\circ}\text{C}$, and the injection volume was 1 μL . The mass spectra were acquired on the Orbitrap ID-X tribrid spectrometer with full scan and targeted MS.² Full scan data were collected in the positive mode from 100 to 600 m/z with a resolution of 30 000 and the targeted MS² data were collected with an isolation window of 0.8 m/z and HCD precursor activation of 40%. The product ions were collected in the Orbitrap at a resolution of 30 000. Inclusion lists including **1a**, **2**, and their respective isotope standards were employed for acquiring the MS² data. The raw data files were processed using Xcalibur 4.3.73.11 (Thermo Fisher Scientific) and manually curated to extract peak areas for the metabolites of interest.

Limit of Detection. The limit of detection (LOD) is defined here as the lowest concentration of a metabolite in a sample detected using the mass spectrometer. Samples of different concentrations for the synthetic **1a** and **2**, ranging from 50 nM to 10 μM , were prepared by serial dilution. Separate calibration curves were generated for **1a** and **2** by plotting the response factor (peak areas) against corresponding metabolite concentrations. The LOD was calculated from the external calibration curves based on the standard deviation of the response (σ) and the slope (s) using the equation; $\text{LOD} = 3.3 * (\sigma/s)$.

Calculations for the Abundance of **1a and **2**.** The ratio of peak areas of endogenous **1a** and **2** to the peak areas of spiked isotopic standards (along y-axis) versus the amount of isotopic standard added per milligram of sponge tissue (along x-axis) were plotted. Data points on these plots were fitted to linear functions. Equating the value of "y" as 1 in the linear equation of the calibration curves for **1a** and **2** delivered their corresponding absolute concentrations in the sponge tissue on the x-axis.

RESULTS AND DISCUSSION

Stereochemical Assignment of **1.** We have previously reported the detection of **1** in *Aplysina*, *Aiolochoxia*, *Stylissa*, and *Ianthella* spp. sponges (Figure 1D, Table 1).^{6,7} However, the stereochemistry at the 1-C α remained indeterminate. A standard for the L-isomer, **1a**, was obtained commercially. The D-isomer, **1b**, was synthesized by guanidinylation of the side chain ϵ -amine of D-lysine. Both standards were derivatized by Marfey's reagent yielding a pair of diastereomers (Figure 2A).

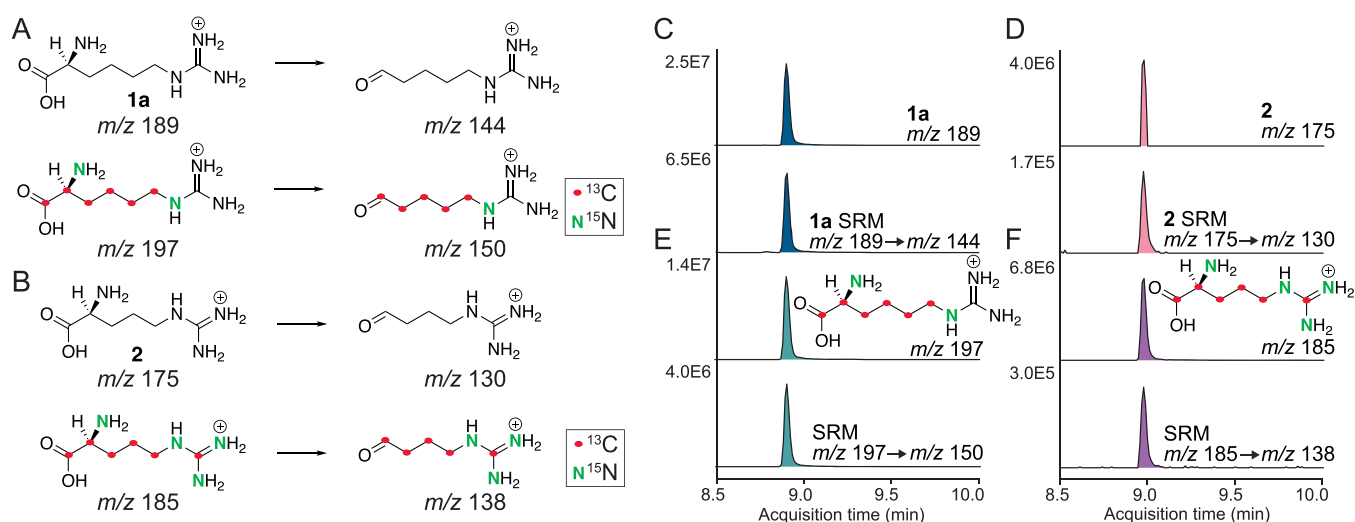


Figure 3. SRM transitions for **1a** and **2**, and their respective isotopic standards. MS¹ parent ions and MS² product ions observed for (A) **1a** and its isotopic standard and (B) **2** and the respective isotopic standard. The MS¹ EIC (top) and SRM chromatogram (bottom) observed for (C) **1a**, (D) **2**, (E) isotopic standard of **1a**, and (F) isotopic standard of **2**. Retention times and peak profiles of the MS¹ EICs are identical to that of the respective SRM chromatograms. ¹³C isotopes are represented as red dots, ¹⁵N isotopes are denoted by green boldface letter "N".

The retention times for derivatized **1a** and **1b** were determined using LC/MS extracted ion chromatograms (EICs, 439.1695 Da ± 0.001 Da) generated from the data collected in the negative ionization mode. Baseline separation between the diastereomers was achieved using reverse-phase chromatography (Figure 2B).

Next, we generated methanolic extracts from sponge tissues and derivatized the extracts with Marfey's reagent. Detection of derivatized **1** in sponge extracts was achieved using identical LC/MS data collection and EIC generation methods that were used for **1a** and **1b** standards. By comparison of retention times, **1a** was identified to be present in all sponge specimens (Figure 2B). The isomer **1b** was not detected. From these data, we conclude that only the L-isomer of **1**, **1a**, is present in marine sponges.

To the best of our knowledge, this is the first experimental determination of the stereochemistry of **1** in marine sponges. The stereochemical assignment based on the data presented in this study is consistent with adducts of **1a** detected with brominated pyrroles in *Agelas* sponges.²¹ It was curious to observe this stereochemical fidelity maintained in the *Ianthella* sp. sponge where **1a** cannot be rationalized to be incorporated into natural products. That the L-isomer **1a** is present in all sponge specimens used in this study likely points toward a similar biogenetic origination mechanism for **1a** in sponges as is operative in humans, which is the guanidinylation of **3**.

Abundance of 1a and 2 in Marine Sponges. To query the absolute abundance of **1a** and **2** in marine sponges, first, we determined the single reaction monitoring (SRM) transitions for these amino acids. A SRM transition refers to the combination of the two *m/z* values; a MS¹ precursor ion *m/z* and the MS² product ion *m/z*.²² The use of SRM transitions provides high selectivity and eliminates contamination with co-eluting or closely eluting isomers which aids in accurate quantification of abundance. The SRM transitions used for **1a** and **2** are illustrated in Figure 3A,B, respectively. For both amino acids, we observed oxidative decarboxylation followed by imine hydrolysis to yield a MS² *Ca*-aldehyde product ion. Thus, for **1a**, the SRM is based on the MS¹ *m/z* 189 → MS² *m/z* 144 transition (Figure 3A). For **2**, the corresponding SRM

is based on the MS¹ *m/z* 175 → MS² *m/z* 130 transition (Figure 3B). For **1a** and **2** standards, EICs for MS¹ *m/z* 189 and MS¹ *m/z* 175 (corresponding to MS¹ ions detected for **1a** and **2**, respectively) and for SRM transitions *m/z* 189 → *m/z* 144 (for **1a**) and *m/z* 175 → *m/z* 130 (for **2**) demonstrated identical retention times and chromatographic profiles (Figure 3C,D), respectively. Next, an isotopic standard for **1a** was synthesized by guanidinylation of commercially available isotopically labeled **3**. An isotopic standard for **2** was commercially obtained. For isotopic standards of **1a** and **2**, EICs for MS¹ *m/z* 197 and MS¹ *m/z* 185 (corresponding to MS¹ ions detected for isotopic standards for **1a** and **2**, respectively) and for SRM transitions *m/z* 197 → *m/z* 150 and *m/z* 185 → *m/z* 138 demonstrated identical retention times and chromatographic profiles (Figure 3E,F), respectively. For sponge extracts, areas under the SRM chromatograms were used for quantification of the abundance of **1a** and **2**.

To minimize matrix effects, different amounts of isotopic standards were directly added to lyophilized and pulverized sponge tissues, followed by extraction and quantification. Assuming identical ionization of **1a** and **2** as compared to their respective isotopic standards, the relative peak area ratios (the SRM chromatogram peak area for **1a** divided by peak area of its isotopic standard; similarly for **2**) were plotted against the concentration of isotopic standard added to the sponge tissue would translate to the abundance of **1a** and **2** in sponge tissues. Using this methodology, the absolute abundance of **1a** and **2** determined in different sponge tissues is illustrated in Figure 4. Calculated LODs for **1a** and **2** were lower than the concentrations of **1a** and **2** detected in sponge tissues used in this study (Figures S11 and S12).

The abundance of the proteinogenic amino acid **2** ranged from the 68.7 ng/mg sponge tissue to 9.1 ng/mg sponge tissue (7.5-fold variation) with the maximum concentration recorded in *Aplysina* sp. and the minimum in *Stylissa* sp. sponge (Figure 4). The variation in the abundance of **1a** was much greater. The highest concentration of **1a** was recorded in *Stylissa* sp. (453.5 ng/mg sponge tissue) and the lowest in *Aplysina* sp.

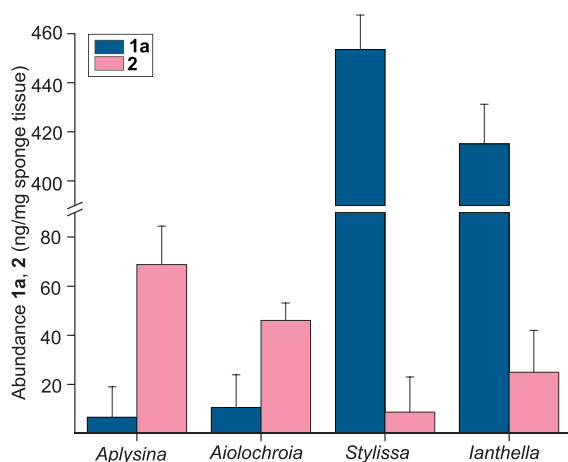


Figure 4. Abundance of **1a** and **2** in *Aplysina*, *Aiolochoiria*, *Stylissa*, and *Ianthella* spp. sponges presented as nanograms of metabolite present per milligram of dried sponge biomass. Histograms represent means from three biological replicates for each sponge species and error bars represent standard deviation in amino acid abundances.

(6.7 ng/mg sponge tissue; 67.6-fold variation). Although the presence of **1a** in *Aplysina* and *Stylissa*, and *Aiolochoiria* spp. sponges can be rationalized based on the respective natural product chemistries, we were surprised to detect the high concentration of **1a** in *Ianthella* sp. (415.1 ng/mg sponge tissue). *Ianthella* sp. does not possess natural products that can be rationalized to be derived from **1a**.

The ratio of concentration of **2** to **1a** in marine sponge samples used in our study ranges from 10.3 in *Aplysina* sp. to 0.02 in *Stylissa* sp. These ratios are in sharp contrast to the human blood plasma and peripheral blood mononuclear cells where **2** dominates **1a** 50- to 300-fold.²³ It is not immediately clear why the *Ianthella* sponge possesses high concentrations of **1a**. Myriad nonproteinogenic amino acids either participate in natural product biosynthetic schemes¹⁶ or are employed in core metabolic and signaling pathways. Although it is apparent that the high abundance of **1a** in the *Ianthella* sp. sponge does not support the biosynthesis of natural products, other roles that **1a** could serve in the physiology of this sponge are not immediately clear. It is tantalizing then to revisit the participation of **1** in NO production. NO in marine sponges is proposed to play fundamental roles in sponge larval settlement and metamorphosis.²⁴ Substrates for NO production, such as **2**, in sponges can be synthesized by symbiotic bacteria associated with the sponge host.²⁵ In low microbial abundance sponges such as *Ianthella* sp.,^{7,26} supplementation of NO production using **1a** may be especially relevant to sponge physiology.

CONCLUSIONS

In this study, we report that only a single isomer of the nonproteinogenic amino acid homoarginine exists in marine sponges. By derivatization with Marfey's reagent and comparison with authentic standards, this isomer was determined to be the L-isomer. We find that the abundance of L-homoarginine amino acid in marine sponges is not strictly correlated with the presence of secondary metabolite natural products into which this amino acid is conceivably incorporated. Some sponges were found to contain a much higher concentration of homoarginine relative to the proteinogenic amino acid arginine. Arginine and homoarginine

are both substrates for the production of NO, a metabolite with important consequences on marine invertebrate physiology and development. This study provides the framework for further investigating the biosynthesis and role of L-homoarginine in marine sponge holobionts.

ASSOCIATED CONTENT

Supporting Information

The Supporting Information is available free of charge at <https://pubs.acs.org/doi/10.1021/acsomega.1c05685>.

Nuclear magnetic resonance spectra and curves demonstrating determination of the abundance of arginine and homoarginine in sponge tissues (PDF)

AUTHOR INFORMATION

Corresponding Author

Vinayak Agarwal – School of Chemistry and Biochemistry and School of Biological Sciences, Georgia Institute of Technology, Atlanta, Georgia 30332, United States; orcid.org/0000-0002-2517-589X; Email: vagarwal@gatech.edu

Authors

Ipsita Mohanty – School of Chemistry and Biochemistry, Georgia Institute of Technology, Atlanta, Georgia 30332, United States
 Samuel G. Moore – School of Chemistry and Biochemistry, Georgia Institute of Technology, Atlanta, Georgia 30332, United States
 Jason S. Biggs – University of Guam Marine Laboratory, Mangilao, Guam 96923, United States
 Christopher J. Freeman – Department of Biology, College of Charleston, Charleston, South Carolina 29424, United States; Smithsonian Marine Station, Ft. Pierce, Florida 34949, United States
 David A. Gaul – School of Chemistry and Biochemistry, Georgia Institute of Technology, Atlanta, Georgia 30332, United States
 Neha Garg – School of Chemistry and Biochemistry, Georgia Institute of Technology, Atlanta, Georgia 30332, United States

Complete contact information is available at: <https://pubs.acs.org/10.1021/acsomega.1c05685>

Notes

The authors declare no competing financial interest.

ACKNOWLEDGMENTS

The authors acknowledge support from the National Science Foundation (NSF, CHE-2004030), the National Institutes of Health (NIH, GM142882), and the Research Corporation for Science Advancement to V.A. and support from the Georgia Institute of Technology's Systems Mass Spectrometry Core Facility.

REFERENCES

- (1) Adams, S.; Che, D.; Qin, G.; Farouk, M. H.; Hailong, J.; Rui, H. Novel biosynthesis, metabolism and physiological functions of L-homoarginine. *Curr. Protein Pept. Sci.* **2019**, *20*, 184–193.
- (2) Mokhaneli, M. C.; Botha-Le Roux, S.; Fourie, C. M. T.; Böger, R.; Schwedhelm, E.; Mels, C. M. C. L-homoarginine is associated with decreased cardiovascular- and all-cause mortality. *Eur. J. Clin. Invest.* **2021**, *51*, No. e13472.

- (3) Pilz, S.; Meinitzer, A.; Gaksch, M.; Grübler, M.; Verheyen, N.; Drechsler, C.; Hartaigh, B. ó.; Lang, F.; Alesutan, I.; Voelkl, J.; März, W.; Tomaschitz, A. Homoarginine in the renal and cardiovascular systems. *Amino Acids* **2015**, *47*, 1703–1713.
- (4) Khalil, A.; Hardman, L.; Ó'Brien, P. The role of arginine, homoarginine and nitric oxide in pregnancy. *Amino Acids* **2015**, *47*, 1715–1727.
- (5) Davids, M.; Ndika, J. D. T.; Salomons, G. S.; Blom, H. J.; Teerlink, T. Promiscuous activity of arginine:glycine amidinotransferase is responsible for the synthesis of the novel cardiovascular risk factor homoarginine. *FEBS Lett.* **2012**, *586*, 3653–3657.
- (6) Mohanty, I.; Moore, S. G.; Yi, D.; Biggs, J. S.; Gaul, D. A.; Garg, N.; Agarwal, V. Precursor-guided mining of marine sponge metabolomes lends insight into biosynthesis of pyrrole–imidazole alkaloids. *ACS Chem. Biol.* **2020**, *15*, 2185–2194.
- (7) Mohanty, I.; Tapadar, S.; Moore, S. G.; Biggs, J. S.; Freeman, C. J.; Gaul, D. A.; Garg, N.; Agarwal, V. Presence of bromotyrosine alkaloids in marine sponges is independent of metabolomic and microbiome architectures. *mSystems* **2021**, *6*, No. e01387.
- (8) Paul, V. J.; Freeman, C. J.; Agarwal, V. Chemical ecology of marine sponges: new opportunities through “-omics”. *Integr. Comp. Biol.* **2019**, *59*, 765–776.
- (9) Han, B.-N.; Hong, L.-L.; Gu, B.-B.; Sun, Y.-T.; Wang, J.; Liu, J.-T.; Lin, H.-W. Natural products from sponges. In *Symbiotic Microbiomes of Coral Reefs Sponges and Corals*; Li, Z., Ed.; Springer Netherlands: Dordrecht, 2019, pp 329–463.
- (10) Peng, J.; Li, J.; Hamann, M. T. The marine bromotyrosine derivatives. *Alkaloids: Chem. Biol.* **2005**, *61*, 59–262.
- (11) Rodríguez, A. D.; Piña, I. C. The structures of aplysinamisines I, II, and III: new bromotyrosine-derived alkaloids from the Caribbean sponge *Aplysina cauliformis*. *J. Nat. Prod.* **1993**, *56*, 907–914.
- (12) Gunasekera, M.; Gunasekera, S. P. Dihydroxyaerthionin and aerophobin 1. Two brominated tyrosine metabolites from the deep water marine sponge *Verongula rigida*. *J. Nat. Prod.* **1989**, *52*, 753–756.
- (13) Al-Mourabit, A.; Zancanella, M. A.; Tilvi, S.; Romo, D. Biosynthesis, asymmetric synthesis, and pharmacology, including cellular targets, of the pyrrole-2-aminoimidazole marine alkaloids. *Nat. Prod. Rep.* **2011**, *28*, 1229–1260.
- (14) Genta-Jouve, G.; Cachet, N.; Holderith, S.; Oberhänsli, F.; Teyssié, J.-L.; Jeffree, R.; Al Mourabit, A.; Thomas, O. P. New insight into marine alkaloid metabolic pathways: revisiting oroidin biosynthesis. *ChemBioChem* **2011**, *12*, 2298–2301.
- (15) Genta-Jouve, G.; Thomas, O. P. Biosynthesis in marine sponges: the radiolabelling strikes back. *Phytochem. Rev.* **2013**, *12*, 425–434.
- (16) Hedges, J. B.; Ryan, K. S. Biosynthetic pathways to nonproteinogenic α -amino acids. *Chem. Rev.* **2020**, *120*, 3161–3209.
- (17) Mohanty, I.; Podell, S.; Biggs, S. J.; Garg, N.; Allen, E. E.; Agarwal, V. Multi-omic profiling of *Melophlus* sponges reveals diverse metabolomic and microbiome architectures that are non-overlapping with ecological neighbors. *Mar. Drugs* **2020**, *18*, 124.
- (18) Dunham, N. P.; Chang, W.-c.; Mitchell, A. J.; Martinie, R. J.; Zhang, B.; Bergman, J. A.; Rajakovich, L. J.; Wang, B.; Silakov, A.; Krebs, C.; Boal, A. K.; Bollinger, J. M. Two distinct mechanisms for C–C desaturation by iron(II)- and 2-(oxo)glutarate-dependent oxygenases: importance of α -heteroatom assistance. *J. Am. Chem. Soc.* **2018**, *140*, 7116–7126.
- (19) Shao, H.; Seifert, J.; Romano, N. C.; Gao, M.; Helmus, J. J.; Jaroniec, C. P.; Modarelli, D. A.; Parquette, J. R. Amphiphilic self-assembly of an N-type nanotube. *Angew. Chem., Int. Ed.* **2010**, *49*, 7688–7691.
- (20) Fujii, K.; Ikai, Y.; Mayumi, T.; Oka, H.; Suzuki, M.; Harada, K.-i. A Nonempirical method using LC/MS for determination of the absolute configuration of constituent amino acids in a peptide: elucidation of limitations of Marfey's method and of its separation mechanism. *Anal. Chem.* **1997**, *69*, 3346–3352.
- (21) Lindel, T.; Hochgürtel, M.; Assmann, M.; Köck, M. Synthesis of the marine natural product $N\alpha$ -(4-bromopyrrolyl-2-carbonyl)-l-homoarginine, a putative biogenetic precursor of the pyrrole–imidazole alkaloids. *J. Nat. Prod.* **2000**, *63*, 1566–1569.
- (22) Holman, S. W.; Sims, P. F. G.; Eyers, C. E. The use of selected reaction monitoring in quantitative proteomics. *Bioanalysis* **2012**, *4*, 1763–1786.
- (23) Davids, M.; Teerlink, T. Plasma concentrations of arginine and asymmetric dimethylarginine do not reflect their intracellular concentrations in peripheral blood mononuclear cells. *Metabolism* **2013**, *62*, 1455–1461.
- (24) Ueda, N.; Richards, G. S.; Degnan, B. M.; Kranz, A.; Adamska, M.; Croll, R. P.; Degnan, S. M. An ancient role for nitric oxide in regulating the animal pelagobenthic life cycle: evidence from a marine sponge. *Sci. Rep.* **2016**, *6*, 37546.
- (25) Song, H.; Hewitt, O. H.; Degnan, S. M. Arginine biosynthesis by a bacterial symbiont enables nitric oxide production and facilitates larval settlement in the marine-sponge host. *Curr. Biol.* **2021**, *31*, 433–437.
- (26) Moitinho-Silva, L.; Steinert, G.; Nielsen, S.; Haridoim, C. C. P.; Wu, Y.-C.; McCormack, G. P.; López-Legentil, S.; Marchant, R.; Webster, N.; Thomas, T.; Hentschel, U. Predicting the HMA-LMA status in marine sponges by machine learning. *Front. Microbiol.* **2017**, *8*, 752.